

Polarized X-Ray Emission from Magnetized Neutron Stars: Signature of Strong-Field Vacuum Polarization

Dong Lai and Wynn C.G. Ho

Center for Radiophysics and Space Research, Department of Astronomy, Cornell University, Ithaca, NY 14853

In the atmospheric plasma of a strongly magnetized neutron star, vacuum polarization can induce a MSW-like resonance across which a X-ray photon may (depending on its energy) convert from one mode into the other, with significant changes in opacities and polarizations. We show that this vacuum resonance effect gives rise to a unique energy-dependent polarization signature in the surface emission from neutron stars: for “normal” field strengths ($10^{12} \lesssim B \lesssim 7 \times 10^{13}$ G), the plane of linear polarization at photon energy $E \lesssim 1$ keV is perpendicular to that at $E \gtrsim 4$ keV, while for “superstrong” field strengths ($B \gtrsim 7 \times 10^{13}$ G), the polarization planes at different energies coincide. The detection of polarized X-rays from neutron stars can provide a direct probe of strong-field quantum electrodynamics and constrain the neutron star magnetic field and geometry.

Surface emission from isolated neutron stars (radio pulsars and radio quiet neutron stars, including magnetars [1]) provides an useful probe of the neutron star (NS) interior physics, surface magnetic fields, and composition. The advent of X-ray telescopes in recent years has made the detection and detailed study of NS surface emission a reality [2]. On the other hand, X-ray emission from accreting X-ray pulsars has long yielded information on the dynamics of accretion and radiative mechanisms in the strong gravity, strong magnetic field regime [3].

In the magnetized plasma that characterizes NS atmospheres, X-ray photons propagate in two normal modes: the ordinary mode (O-mode) is mostly polarized parallel to the \mathbf{k} - \mathbf{B} plane, while the extraordinary mode (X-mode) is mostly polarized perpendicular to the \mathbf{k} - \mathbf{B} plane, where \mathbf{k} is the photon wave vector and \mathbf{B} is the external magnetic field [3]. This description of normal modes applies under typical conditions, when the photon energy E is much less than the electron cyclotron energy $E_{Be} = \hbar e B / (m_e c) = 11.6 B_{12}$ keV [where $B_{12} = B / (10^{12} \text{ G})$], E is not too close to the ion cyclotron energy $E_{Bi} = 6.3 B_{12} (Z/A)$ eV (where Z and A are the charge number and mass number of the ion), the plasma density is not too close to the vacuum resonance (see below) and θ_{kB} (the angle between \mathbf{k} and \mathbf{B}) is not close to zero. Under these conditions, the X-mode opacity (due to scattering and absorption) is greatly suppressed compared to the O-mode opacity, $\kappa_X \sim (E/E_{Be})^2 \kappa_O$ [3, 4]. As a result, the X-mode photons escape from deeper, hotter layers of the NS atmosphere than the O-mode photons, and the emergent radiation is linearly polarized to a high degree (as high as 100%) [5, 6, 7]. Measurements of X-ray polarization, particularly when phase-resolved and measured in different energy bands, could provide unique constraints on the magnetic field strength and geometry and the compactness of the NS [6, 7, 8].

It has long been predicted from quantum electrodynamics (QED) that in a strong magnetic field the vacuum becomes birefringent [9, 10, 11, 12, 13]. Acting by itself, the birefringence from vacuum polarization is significant (with the index of refraction differing from unity by more than 10%) only for $B \gtrsim 300 B_Q$, where

$B_Q = m_e^2 c^3 / (e \hbar) = 4.414 \times 10^{13}$ G is the critical QED field strength. However, when combined with the birefringence due to the magnetized plasma, vacuum polarization can greatly affect radiative transfer at much smaller field strengths. A “vacuum resonance” arises when the contributions from the plasma and vacuum polarization to the dielectric tensor “compensate” each other [14, 15, 17]. For a photon of energy E , the vacuum resonance occurs at the density $\rho_V \simeq 9.64 \times 10^{-5} Y_e^{-1} B_{12}^2 E_1^2 f^{-2} \text{ g cm}^{-3}$, where Y_e is the electron fraction, $E_1 = E / (1 \text{ keV})$, and $f = f(B)$ is a slowly varying function of B and is of order unity ($f = 1$ for $B \ll B_Q$ and $f \rightarrow (B/5B_Q)^{1/2}$ for $B \gg B_Q$; see refs. [17, 18]). For $\rho > \rho_V$ (where the plasma effect dominates the dielectric tensor) and $\rho < \rho_V$ (where vacuum polarization dominates), the photon modes (for $E \ll E_{Be}$, $E \neq E_{Bi}$ and $\theta_{kB} \neq 0$) are almost linearly polarized; near $\rho = \rho_V$, however, the normal modes become circularly polarized as a result of the “cancellation” of the plasma and vacuum effects — both effects tend to make the mode linearly polarized, but in mutually orthogonal directions. When a photon propagates in an inhomogeneous medium, its polarization state will evolve adiabatically (i.e. following the K_+ or K_- curve in Fig. 1) if the density variation is sufficiently gentle. Thus, a X-mode (O-mode) photon will be converted into the O-mode (X-mode) as it traverses the vacuum resonance, with its polarization ellipse rotated by 90° (Fig. 1). This resonant mode conversion is analogous to the Mikheyev-Smirnov-Wolfenstein neutrino oscillation that takes place in the Sun [19, 20]. For this conversion to be effective, the adiabatic condition must be satisfied [17, 21] (cf. [16])

$$E \gtrsim E_{\text{ad}} = 2.52 (f \tan \theta_{kB} |1 - u_i|)^{2/3} \left(\frac{1 \text{ cm}}{H_\rho} \right)^{1/3} \text{ keV}, \quad (1)$$

where $u_i = (E_{Bi}/E)^2$ and $H_\rho = |dz/d \ln \rho|$ is the density scale height (evaluated at $\rho = \rho_V$) along the ray. For an ionized Hydrogen atmosphere, $H_\rho \simeq 2kT / (m_p g \cos \theta) = 1.65 T_6 / (g_{14} \cos \theta) \text{ cm}$, where $T = 10^6 T_6 \text{ K}$ is the temperature, $g = 10^{14} g_{14} \text{ cm s}^{-2}$ is the gravitational acceleration, and θ is the angle between the ray and the surface

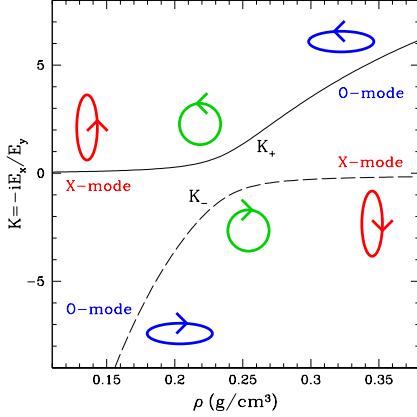


FIG. 1: The polarization ellipticity of the photon mode as a function of density near the vacuum resonance. The two curves correspond to the two different modes. In this example, the parameters are $B = 10^{13}$ G, $E = 5$ keV, $Y_e = 1$, and $\theta_{kB} = 45^\circ$. The ellipticity of a mode is specified by the ratio $K = -iE_x/E_y$, where E_x (E_y) is the photon's electric field component along (perpendicular to) the \mathbf{k} - \mathbf{B} plane. The O-mode is characterized by $|K| \gg 1$, and the X-mode $|K| \ll 1$.

normal. In general, the mode conversion probability is given by [17, 21]

$$P_{\text{con}} = 1 - \exp[-(\pi/2)(E/E_{\text{ad}})^3]. \quad (2)$$

The probability for a nonadiabatic “jump” is $(1 - P_{\text{con}})$.

Because the two photon modes have vastly different opacities, the vacuum resonance can significantly affect the transfer of photons in NS atmospheres. When the vacuum polarization effect is neglected, the decoupling densities of the O-mode and X-mode photons (i.e., the densities of their respective photospheres, where the optical depth measured from outside is $2/3$) are approximately given by (for Hydrogen plasma and θ_{kB} not too close to 0) $\rho_O \simeq 0.42 T_6^{-1/4} E_1^{3/2} G^{-1/2} \text{ g cm}^{-3}$ and $\rho_X \simeq 486 T_6^{-1/4} E_1^{1/2} B_{14} G^{-1/2} \text{ g cm}^{-3}$, where $G = 1 - e^{-E/kT}$ [17]. There are two different magnetic field regimes: For “normal” magnetic fields,

$$B < B_l \simeq 6.6 \times 10^{13} T_6^{-1/8} E_1^{-1/4} G^{-1/4} \text{ G}, \quad (3)$$

the vacuum resonance lies outside both photospheres ($\rho_V < \rho_O, \rho_X$); for the magnetar field regime, $B > B_l$, the vacuum resonance lies between these two photospheres, i.e., $\rho_O < \rho_V < \rho_X$ (the condition $\rho_V < \rho_X$ is satisfied for all field strengths and relevant energies and temperatures). These two field regimes yield qualitatively different X-ray polarization signals.

Consider the “normal” field strengths, $10^{12} \text{ G} \lesssim B \lesssim B_l$, which apply to most NSs (see Fig. 2). In this regime,

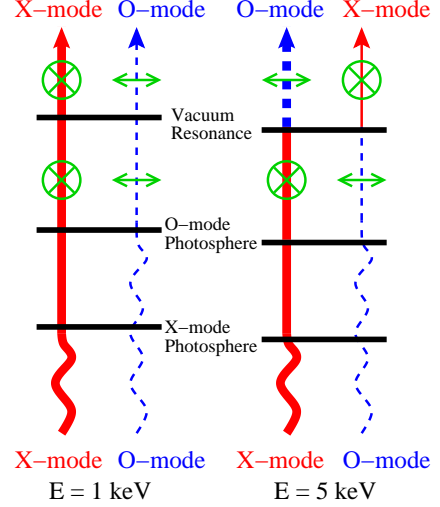


FIG. 2: A schematic diagram illustrating how vacuum polarization affects the polarization state of the emergent radiation from a magnetized NS atmosphere. This diagram applies to the “normal” field regime [$B \lesssim 7 \times 10^{13}$ G, see eq. (3)] in which the vacuum resonance lies outside the photospheres of the two photon modes. The photosphere is defined where the optical depth (measured from outside) is $2/3$ and is where the photon decouples from the matter. At low energies (such as $E \lesssim 1$ keV), the photon evolves nonadiabatically across the vacuum resonance (for θ_{kB} not too close to 0), and thus the emergent radiation is dominated by the X-mode. At high energies ($E \gtrsim 4$ keV), the photon evolves adiabatically, with its plane of polarization rotating by 90° across the vacuum resonance, and thus the emergent radiation is dominated by the O-mode. The plane of linear polarization at low energies is therefore perpendicular to that at high energies.

the atmosphere structure and total spectrum can be calculated without including vacuum polarization [to be more accurate, we require $(B/B_l)^4 \ll 1$ for this to be valid]. For concreteness, we consider emission from a hot spot (magnetic polar cap) on the NS; the magnetic field at the hot spot (with size much smaller than the stellar radius) is perpendicular to the stellar surface. Let the specific intensities of the O-mode and X-mode emerging from their respective photospheres (which lie below the vacuum resonance) be $I_O^{(0)}$ and $I_X^{(0)}$, which we calculate using our H atmosphere models developed previously [18, 22]. For a given B and T_{eff} , both $I_O^{(0)}$ and $I_X^{(0)}$ depend on E and θ_{kB} at emission (the hot spot). As the radiation crosses the vacuum resonance, the intensities of the O-mode and X-mode become $I_O = (1 - P_{\text{con}})I_O^{(0)} + P_{\text{con}}I_X^{(0)}$ and $I_X = (1 - P_{\text{con}})I_X^{(0)} + P_{\text{con}}I_O^{(0)}$. In calculating P_{con} , we use the temperature profile of the atmosphere model to determine the density scale height at the vacuum resonance. We note that in principle, circular polarization can be produced when a photon crosses the vacuum resonance [21], but the net circular polarization is expected to be zero when photons from a finite-

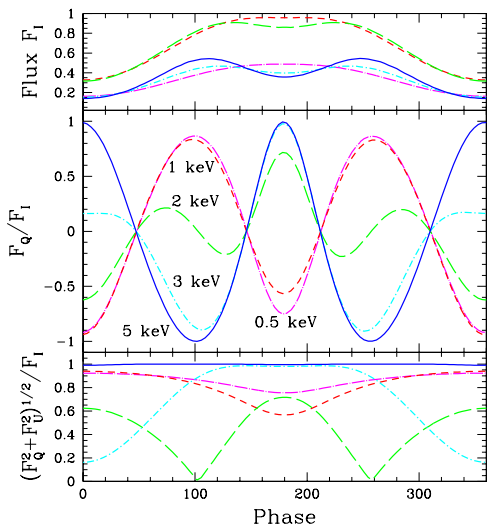


FIG. 3: The phase evolution of the observed spectral flux (upper panel, in arbitrary units), the linear polarization F_Q/F_I (middle panel) and the polarization degree $P_L = (F_Q^2 + F_U^2)^{1/2}/F_I$ (lower panel) produced by the magnetic polar cap of a rotating NS. The model parameters are: the magnetic field $B = 10^{13}$ G, the effective temperature of the polar cap $T_{\text{eff}} = 5 \times 10^6$ K, the angle between the spin axis and the line-of-sight $\gamma = 30^\circ$ and the angle between the magnetic axis and spin axis $\beta = 70^\circ$. The different curves are for different photon energies as labeled. In the upper panel, the flux at 5 keV has been multiplied by 10 relative to the other curves. The definition of the Stokes parameter is such that $F_Q/F_I = 1$ corresponds to linear polarization in the plane spanned by the line-of-sight vector and the star’s spin axis (the zero phase corresponds to the polar cap in the same plane). Note that the polarization plane of high-energy ($E \gtrsim 4$ keV) photons is perpendicular to that of low-energy photons ($E \lesssim 1$ keV). Also note that for E around E_{ad} , the polarization degree P_L can be zero at certain phases such that $P_{\text{con}} = 1/2$.

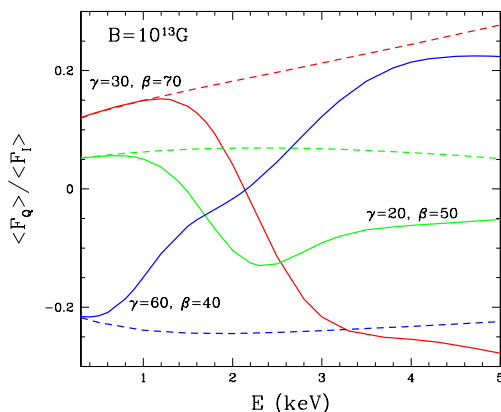


FIG. 4: The phase-averaged linear polarization as a function of photon energy. The model parameters are $B = 10^{13}$ G and $T_{\text{eff}} = 5 \times 10^6$ K, and the three curves correspond to three different sets of angles (γ, β) as labeled. The averaged $\langle F_U \rangle = 0$. The dashed curves depict the results when the vacuum polarization effect is turned off.

sized polar cap are taken into account.

To determine the observed polarization, we must consider propagation of polarized radiation in the NS magnetosphere, whose dielectric property in the X-ray band is dominated by vacuum polarization [8]. As a photon (of a given mode) propagates from the polar cap through the magnetosphere, its polarization state evolves adiabatically following the varying magnetic field it experiences, up to the “polarization-limiting radius” r_{pl} , beyond which the polarization state is frozen. We set up a fixed coordinate system XYZ , where the Z -axis is along the line-of-sight and the X -axis lies in the plane spanned by the Z -axis and Ω (the spin angular velocity vector). The direction of the magnetic field \mathbf{B} following the photon trajectory in this coordinate system is specified by the polar angle $\theta_B(s)$ and the azimuthal angle $\phi_B(s)$ (where s is the affine parameter along the ray). The X, Y -components of the electric field of the photon mode are $(E_X, E_Y) = (\cos \phi_B, \sin \phi_B)$ for the O-mode and $(-\sin \phi_B, \cos \phi_B)$ for the X-mode. The adiabatic condition requires $|n_X - n_O| \gtrsim 2(\hbar c/E)|d\phi_B/ds|$ (where n_X, n_O are the indices of refraction of the two modes); this condition breaks down at $r = r_{\text{pl}}$, which is much greater than the stellar radius for all parameter regimes of interest in this paper. The observed Stokes parameters (normalized to the total intensity I) are given by $Q/I = (2P_{\text{con}} - 1)p_e \cos 2\phi_B(r_{\text{pl}})$ and $U/I = (2P_{\text{con}} - 1)p_e \sin 2\phi_B(r_{\text{pl}})$, where $p_e = (I_X^{(0)} - I_O^{(0)})/(I_X^{(0)} + I_O^{(0)})$ is the “intrinsic” polarization fraction at emission, and $\phi_B(r_{\text{pl}})$ is the azimuthal angle of the magnetic field at $r = r_{\text{pl}}$ [For $r_{\text{pl}} \ll c/\Omega$, or for spin frequency $\ll 70$ Hz, $\phi_B(r_{\text{pl}}) \simeq \pi + \phi_B(R)$]. We calculate the observed spectral fluxes F_I, F_Q, F_U (associated with the intensities I, Q, U) using the standard procedure, including the effect of general relativity [23].

Figure 3 shows the total flux and polarization “light curves” generated from the hot polar cap of a rotating NS. As the star rotates, the plane of linear polarization rotates. The light curves obviously depend on the geometry (specified by the angles β and γ). Note that F_Q for low-energy ($E \lesssim 1$ keV) photons is opposite to that for high-energy photons ($E \gtrsim 4$ keV), which implies that the planes of linear polarization at low and high energies are orthogonal. This feature also manifests in the phase-averaged linear polarization (see Fig. 4). This is an unique signature of photon mode conversion induced by vacuum polarization.

In the magnetar field regime, $B > B_l$, the vacuum resonance lies between the photospheres of the two modes. At low energies (e.g., $E \lesssim 1$ keV), no mode conversion occurs at the vacuum resonance, and vacuum polarization makes the X-mode photosphere lie above (i.e. at lower density) its “original” location (i.e. when vacuum polarization is turned off) because the photon opacity exhibits a large spike at the vacuum resonance [17]. At high energies (e.g., $E \gtrsim 4$ keV), the effective X-mode photosphere lies very near the vacuum resonance. For both low and high energies, the emergent radiation is dominated by the

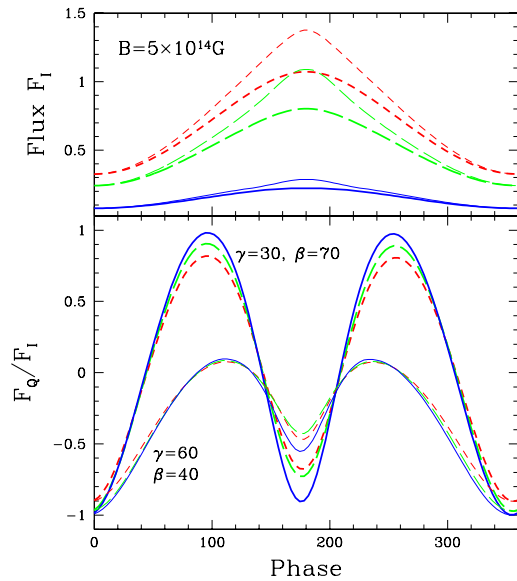


FIG. 5: Same as Fig. 3, except for $B = 5 \times 10^{14}$ G and $T_{\text{eff}} = 5 \times 10^6$ K. The different curves are for different photon energies (1 keV dashed, 2 keV long-dashed, 5 keV solid lines). The thicker curves are for $\gamma = 30^\circ$, $\beta = 70^\circ$, and the thin curves for $\gamma = 60^\circ$, $\beta = 40^\circ$. In contrast to Fig. 3-4, in the magnetar field regime, the planes of linear polarization at different photon energies coincide with each other.

X-mode (for θ_{kB} not too close to 0). Therefore the planes of linear polarization at different energies coincide and evolve “in phase” as the star rotates (see Fig. 5). These polarization signals are qualitatively different from the “normal” field regime. Note that in the magnetar field

regime, vacuum polarization significantly affects the total spectral flux from the atmosphere [17, 18, 21]: (i) Vacuum polarization makes the effective decoupling density of X-mode photons (which carry the bulk of the thermal energy) smaller, thereby depleting the high-energy tail of the spectrum and making the spectrum closer to black-body; (ii) vacuum polarization suppresses the proton cyclotron line and other spectral line features [24] in the spectra by making the decoupling depths inside and outside the line similar. As we discussed in previous papers [18, 24], the absence of lines in the observed thermal spectra of several magnetar candidates [25] may be considered as a proof of the vacuum polarization effect at work in these systems. Measurement of X-ray polarization would provide an independent probe of the magnetic fields of these objects.

Finally, we note that although the specific results shown in Figs. 3-5 refer to emission from a hot polar cap on the NS, we expect the vacuum polarization signature (e.g., that the planes of linear polarization at $E \lesssim 1$ keV and at $E \gtrsim 4$ keV are orthogonal for $B \lesssim 7 \times 10^{13}$ G) to be present in more complicated models (e.g. when several hot spots or the whole stellar surface contribute to the X-ray emission). This is because the polarization-limiting radius (due to vacuum polarization in the magnetosphere) lies far away from the star (see above), where rays originating from different patches of the star experience the same dipole field [8]. Our results therefore demonstrate the unique potential of X-ray polarimetry [26] in probing the physics under extreme conditions (strong gravity and magnetic fields) and the nature of various forms of NSs.

This work was supported by NASA grant NAG 5-12034 and NSF grant AST 0307252.

-
- [1] C. Thompson and R.C. Duncan, *Mon. Not. Roy. Astron. Soc.* 275, 255 (1995).
 - [2] G.G. Pavlov, V.E. Zavlin, and D. Sanwal, in *Neutron Stars, Pulsars, and Supernova Remnants*, edited by W. Becker, et al. (MPI, Garching, 2002), p.273.
 - [3] P. Mészáros, *High-Energy Radiation from Magnetized Neutron Stars* (Univ. Chicago Press, Chicago, 1992).
 - [4] J. Lodenquai, V. Canuto, M. Ruderman., and S. Tsuruta, *Astrophys. J* 190, 141 (1974).
 - [5] Yu.N. Gnedin and R.A. Sunyaev, *Astron. & Astrophys.* 36, 379 (1974).
 - [6] P. Mészáros et al., *Astrophys. J* 324, 1056 (1988).
 - [7] G.G. Pavlov and V.E. Zavlin, *Astrophys. J* 529, 1011 (2000).
 - [8] J.S. Heyl, N.J. Shaviv, and D. Lloyd, *Astrophys. J.* (in press) astro-ph/0302118.
 - [9] W. Heisenberg and H. Euler, *Z. Physik* 98, 714 (1936).
 - [10] J. Schwinger, *Phys. Rev.* 82, 664 (1951).
 - [11] S.L. Adler, *Ann. Phys.* 67, 599 (1971).
 - [12] W.Y. Tsai and T. Erber, *Phys. Rev. D* 12, 1132 (1975).
 - [13] J.S. Heyl and L. Hernquist, *J. Phys. A* 30, 6485 (1997).
 - [14] Yu.N. Gnedin, G.G. Pavlov, and Yu.A. Shibano, *Sov. Astron. Lett.* 4, 117 (1978).
 - [15] P. Mészáros and J. Ventura, *Phys. Rev. D* 19, 3565 (1979).
 - [16] G.G. Pavlov and Yu.N. Gnedin, *Sov. Sci. Rev. E: Astrophys. Space Phys.* 3, 197 (1984).
 - [17] D. Lai and W.C.G. Ho, *Astrophys. J.* 566, 373 (2002).
 - [18] W.C.G. Ho and D. Lai, *Mon. Not. Roy. Astron. Soc.* 338, 233 (2003).
 - [19] W.C. Haxton, *Ann. Rev. Astron. Astrophys.* 33, 459 (1995).
 - [20] J.N. Bahcall, M.C. Gonzalez-Garcia, and C. Pena-Garay, *J. High Energy Phys.* JHEP02, 009, (2003).
 - [21] D. Lai and W.C.G. Ho, *Astrophys. J.* 588, 962 (2003)
 - [22] W.C.G. Ho and D. Lai, *Mon. Not. Roy. Astron. Soc.* 327, 1081 (2001).
 - [23] K.R. Pechenick, C. Ftaclas, and J.M. Cohen, *Astrophys. J.* 274, 846 (1983).
 - [24] W.C.G. Ho, D. Lai, A.Y. Potekhin, and G. Chabrier, *Astrophys. J.* (submitted).
 - [25] A.M. Juett, H.L. Marshall, D. Chakrabarty, and N.S. Schulz, *Astrophys. J. Lett.* 568, L31 (2002).
 - [26] E. Costa et al., *Nature* 411, 662 (2001).